Electronic Supplementary Material (ESI) for Journal of Materials Chemistry A.

Supporting information

Green reduction of graphene oxide by polydopamine to construct flexible film: superior flame retardancy and high thermal conductivity

Fubin Luo [1, 2], Kun Wu [1*], Jun Shi[1, 2], Xiangxiang Du[1, 2], Xiaoya Li[1, 2,3], Liu Yang[1, 2,3], Mangeng Lu[1*]

[1]*Key Laboratory of Cellulose and Lignocellulosics Chemistry, Guangzhou Institute of Chemistry, Chinese Academy of Sciences, Guangzhou 510650, PR China*

[2]*University of Chinese Academy of Sciences, Beijing 100039, PR China*

[3]*Guangdong Provincial Engineering & Technology Research Center for Touch Significant Devices Electronic Materials, Guangzhou 510650, PR China*

1. Preparation of the films

Table 1 the composition of the prepared film

Sample	GO	GPI	GPH	GPF	GPE
Graphene oxide	1.0	9.6	4.8	2.4	1.2
Dopamine	0	1.0	1.0	1.0	1.0

The film is prepared according to the stoichiometric ratio described in Tab. 1. The

* Corresponding author, Tel (Fax): + 86-20-85231925; E-mail address: wukun@gic.ac.cn mglu@gic.ac.cn

reduction of the graphene oxide by dopamine is recorded by XRD, the corresponding patterns are shown in Fig. 1. A sharp peak located at 9.70^{o} of GO can be observed from Fig. 2, which is the typical diffraction peak of GO. According to Bragg's equation, the *d* spacing is 0.91 nm. As the content of the dopamine increases, new diffraction peaks are arouse, and when the stoichiometric ratio of (graphene oxide to dopamine) is decreased to 2.4:1, the typical diffraction peak of GO is completed disappeared, which indicated that the graphene oxide sheets are almost totally transfer to reduced grapnene oxide (rGO).

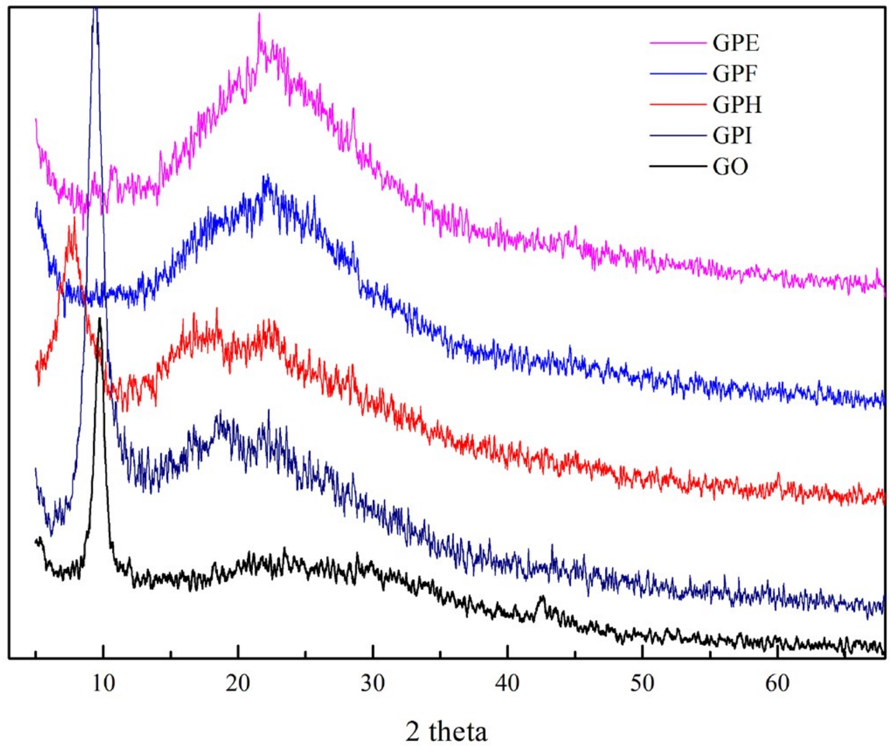

Fig. 1 XRD patterns of series film

2. Effective medium theory

To account for the association between thermal conductive phenomenon and the laminated structure of the film, the effective medium theory is adopted for interpret the thermal resistance[1-3].

$$K_{11} = K_{22} = K_m \frac{2 + f\,[\beta_1 (1 - L_{11})(1 + \langle \cos^2\theta \rangle) + \beta_3 (1 - L_{33})(1 - \langle \cos^2\theta \rangle)]}{2 - f\,[\beta_1 L_{11}(1 + \langle \cos^2\theta \rangle) + \beta_3 L_{33}(1 - \langle \cos^2\theta \rangle)]} \qquad E_{1a}$$

$$K_{33} = K_m \frac{1 + f\,[\beta_1 (1 - L_{11})(1 - \langle \cos^2\theta \rangle) + \beta_3 (1 - L_{33}) \langle \cos^2\theta \rangle]}{1 - f\,[\beta_1 L_{11}(1 - \langle \cos^2\theta \rangle) + \beta_3 L_{33} \langle \cos^2\theta \rangle]} \qquad E_{1b}$$

$$\beta_{ii} = \frac{K_{ii}^{c} - K_m}{K_m + L_{ii}(K_{ii}^{c} - K_m)} \qquad E_2$$

$$\langle \cos^2\theta \rangle = \frac{\int \rho(\theta) \cos^2\theta \sin\theta \, d\theta}{\int \rho(\theta) \sin\theta \, d\theta} \qquad E_3$$

Where K_{11} and K_{22} represent the in-plane thermal conductivities and K_{33} is the across-plane thermal conductivity. θ is the angle between the materials plane and the local particles symmetric axis. $\rho(\theta)$ is a distribution function describing the ellipsoidal particle orientation, f is the volume fraction of the filler, K_{ii}^{c} (i=1, 2, 3) are the equivalent thermal conductivities conductivities along the symmetric axis of this aligned composites unit cell. K_m is the thermal conductivity of the matrix phase, L_{ii} are the geometrical factors dependent on the particle shape and are given by the following equation:

$$L_{11} = L_{22} = \frac{p^2}{2(p^2 - 1)} + \frac{p}{2(1 - p^2)^{3/2}} \cos^{-1} p \qquad \text{for } p < 1 \qquad E_4$$

$$L_{33} = 1 - 2L_{11} \qquad E_5$$

$$K_{ii}^{c} = \frac{K_m K_p}{K_m + (2p + 1)\alpha L_{ii} K_p} \qquad E_6$$

Here a dimensionless parameter, α, is defined by

$$\alpha = \frac{R_{bd} K_m}{h} \qquad E_7$$

Where R_{bd} is thermal boundary resistance and h is the thickness of the nanosheets.

For the laminate composites, considering the aligned graphene, assuming ideal case, $p \to 0$, $L_{11} = 0$ and $L_{33} = 1$. Thus, E_2 and E_6 can be expressed as following:

$$K_{11}^{c} = K_{22}^{c} = Kp \qquad E_8$$

$$K_{33}^{c} = \frac{K_m K_p}{K_m + \alpha K_p} \qquad E_9$$

$$\beta_1 = \frac{K_p - K_m}{K_m} \qquad E_{10}$$

$$\beta_{33} = (1 - \alpha) - \frac{K_m}{K_p} \qquad E_{11}$$

Thus equations of effective medium theory reduce to:

$$K_{11} = K_{22} = K_m \frac{2 + f\left[\frac{K_p}{K_m}\left(1 + <\cos^2\theta>\right)\right]}{2 - f\left[\frac{K_p h - K_m h - R_{bd} K_p K_m}{K_p h}\left(1 - <\cos^2\theta>\right)\right]} \qquad E_{12}$$

$$K_{33} = K_m \frac{1 + f\left[\frac{K_p}{K_m}\left(1 - <\cos^2\theta>\right)\right]}{1 - f\left[\frac{K_p h}{h + R_{bd} K_p}\left(\cos^2\theta\right)\right]} \qquad E_{13}$$

Where K_m is the thermal conductivity of the matrix phase, K_p is the thermal conductivity of the laminated nanosheets, f is the volume fraction of the particles, θ is the angle betweenthe materials axis, X_3, and the local particles symmetric axis, R_{bd} is thermal boundary resistance, and h is the thickness of the reduced graphene.

In the case of GPF, from the sectional SEM image, Materials axis X_3 is perpendicular to to the graphene sheets symmetric axis (X_1 and X_2 direction), which means that θ is tend to be zero. Thus, Rbd can be expressed as:

$$R_{bd} = \left(\frac{f\, K_{33}}{K_{33} - K_m} - \frac{1}{K_p}\right) h$$

In this case, h is approximately 0.5 nm, K_{33} is 0.69 W m^{-1} k^{-1}, and it can be approximatively calculated that R_{bd} is less than 0.5×10^{-9} $K\cdot m^2\cdot W^{-1}$ [4-5].

of charred layer of GPF(d)(e)

3. π-π stacking

The XRD pattern of GPF shown in Fig. 2 in the papers demonstrate the reduction of the GO. In detail, the peaks in the curve can be collected (2Θ=17.76, 20.40, 21.88, 22.24, 25.64 and 28.50), respectively, the corresponding *d* spacing are 0.500, 0.435, 0.406, 0.399, 0.347, 0.312nm. The narrow spacing might be aroused by the π-π stacking between the reduced GO and polydopamine[6-7].

4. Tensile strength of the prepared films

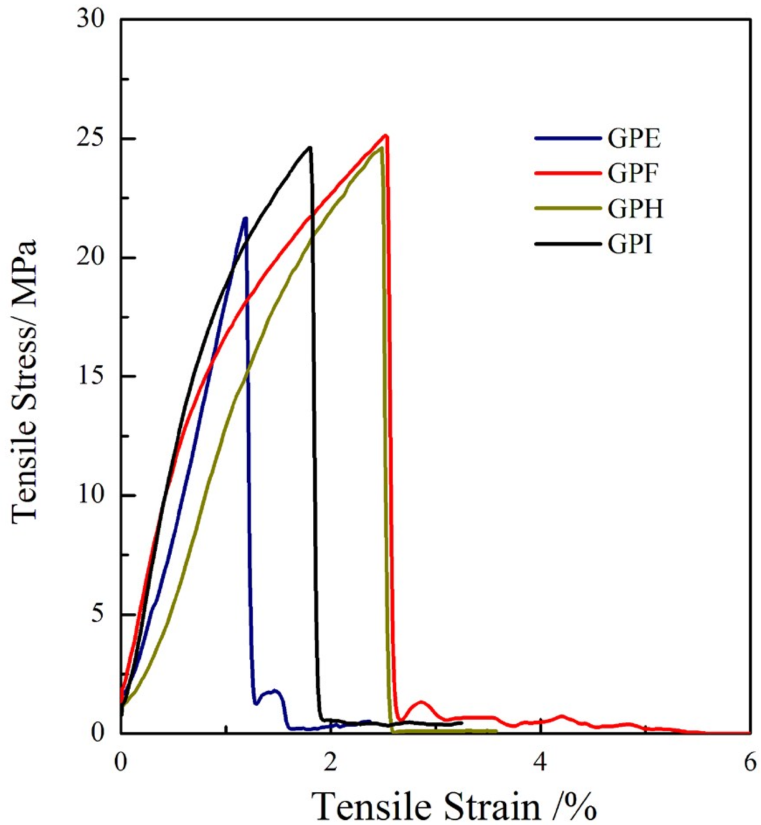

Fig. 2 Strain-stress curves of the prepared films

The strain stress curves of the prepared films are presented in Fig. 2. It can be observed that the tensile strength of the films shows little difference. The tensile strength of GPE, GPF,GPH,GPI is 24.5, 25.0, 24.4 and 21.6 respectively. Among these films, GPE get a relative low tensile strength, which may be aroused by the totally reduction of the GO, which impairs the hydrogen bond between the rGO sheets and polydopamine.

5. Fire performance of the prepared films

The fire performances of the prepared films are depicted in Fig. 4. It can be found that all the films have excellent flame retardancy. However, based on the digital images of the samples after fire tests shown in Fig. 5, the flame stability of the film varies as the compositions of the film. Due to the less content of polydopamine, GPH and GPI can be burnt out, by leaving the large holes. This phenomenon demonstrates that polydopamine play a significant role in the flame retardant of the film.

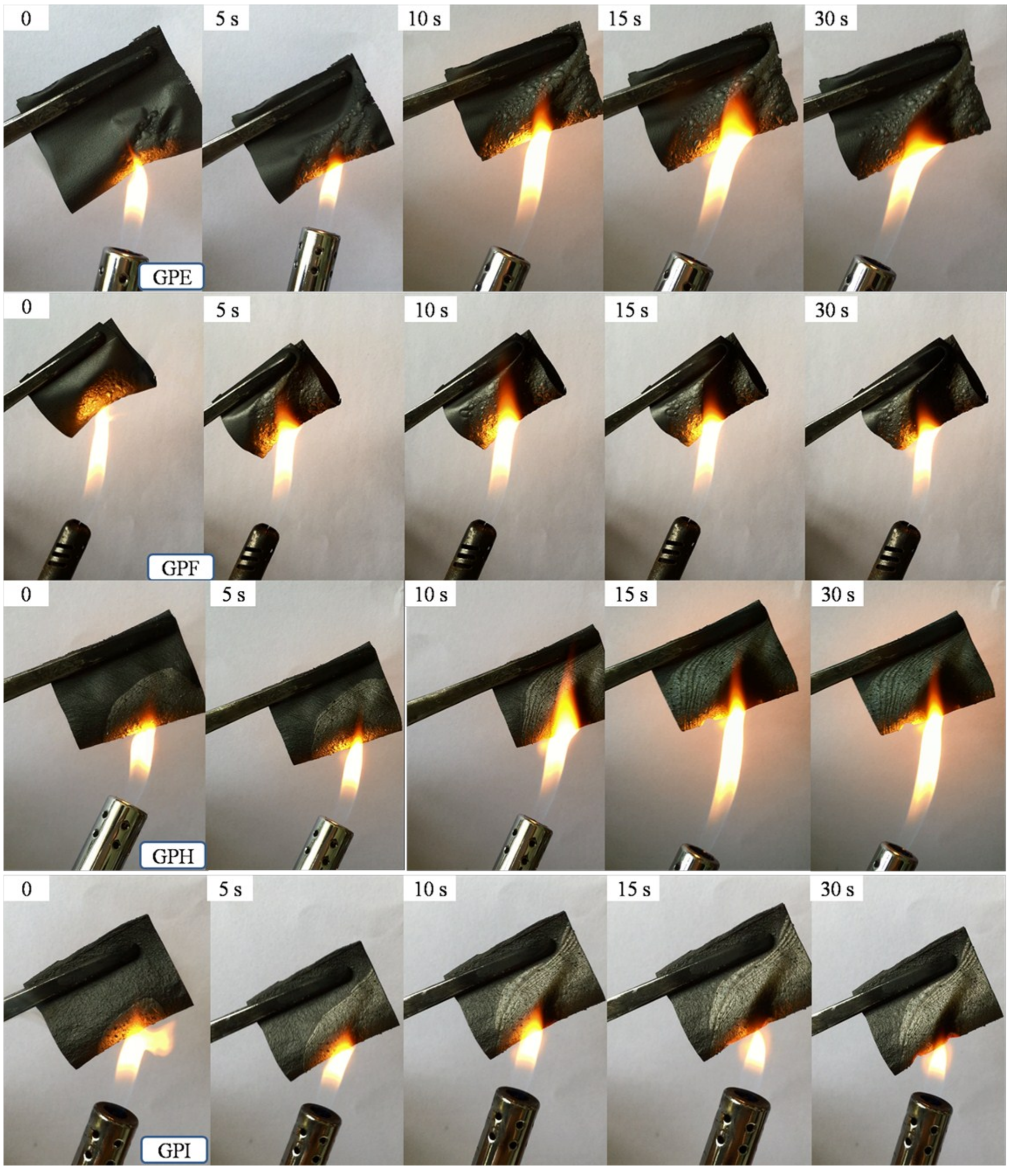

Fig. 3 Fire performance of the prepared films

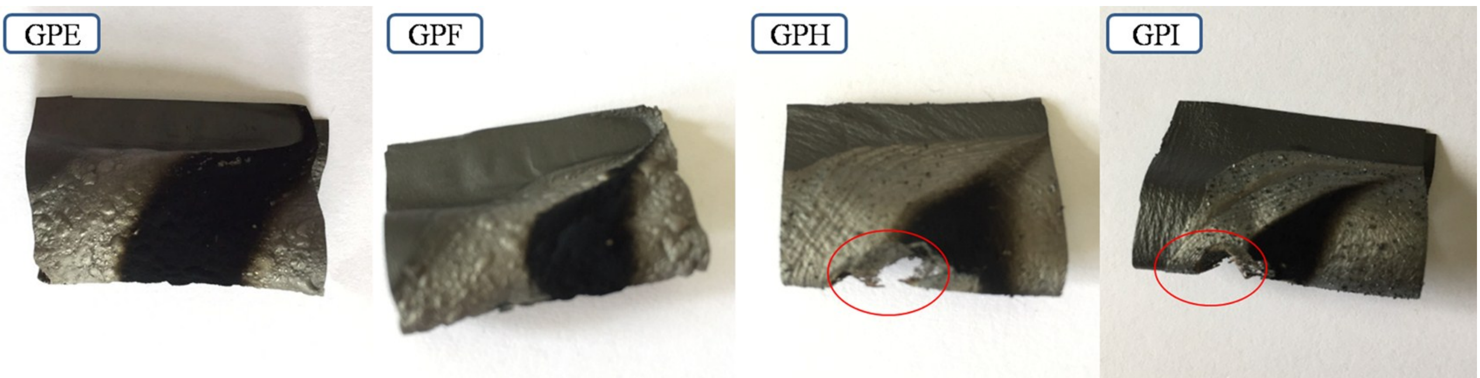

Fig. 3 Digital images of The samples after fire tests

References

(1). Li, Q.; Guo, Y.; Li, W.; Qiu, S.; Zhu, C.; Wei, X.; Chen, M.; Liu, C.; Liao, S.; Gong, Y., Ultrahigh Thermal Conductivity of Assembled Aligned Multilayer Graphene/Epoxy Composite. *Chem. Mater.* **2014,** *26* 4459-4465.

(2). Nan, C. W.; Birringer, R.; Clarke, D. R.; Gleiter, H., Effective thermal conductivity of particulate composites with interfacial thermal resistance. *J. Appl. Phys.* **1997,** *81* 6692-6699.

(3). Song, N.; Jiao, D.; Ding, P.; Cui, S.; Tang, S.; Shi, L., Anisotropic thermally conductive flexible films based on nanofibrillated cellulose and aligned graphene nanosheets. *Journal of Materials Chemistry C* **2015,** *4* 305-314.

(4). Faugeras, C.; Faugeras, B.; Orlita, M.; Potemski, M.; Nair, R. R.; Geim, A. K., Thermal conductivity of graphene in corbino membrane geometry. *Acs Nano* **2010,** *4* 1889-92.

(5). Konatham, D.; Papavassiliou, D. V.; Striolo, A., Thermal boundary resistance at the graphene–graphene interface estimated by molecular dynamics simulations. *Chem. Phys. Lett.* **2012,** *527* 47-50.

(6). Główka, M. L.; Martynowski, D.; Kozłowska, K., Stacking of six-membered aromatic rings in crystals. *J. Mol. Struct.* **1999,** *474* 81–89.

(7). Dreyer, D. R.; Miller, D. J.; Freeman, B. D.; Paul, D. R.; Bielawski, C. W., Elucidating the structure of poly(dopamine). *Langmuir the Acs Journal of Surfaces & Colloids* **2012,** *28* 6428-35.